J|A|C|S
ARTICLES
Published on Web 07/31/2002

Conformational Preferences of Jet-Cooled Melatonin: Probing *trans*- and *cis*-Amide Regions of the Potential Energy Surface

Gina M. Florio,[†] Richard A. Christie,[‡] Kenneth D. Jordan,[‡] and Timothy S. Zwier*,[†]

Contribution from the Department of Chemistry, Purdue University, West Lafayette, Indiana 47907-1393, and the Department of Chemistry, University of Pittsburgh, Pittsburgh, Pennsylvania 15260

Received April 18, 2002

Abstract: The hormone melatonin (*N*-acetyl-5-methoxytryptamine) is an indole derivative with a flexible peptide-like side chain attached at the C3 position. Using a combination of two-color resonant two-photon ionization (2C-R2PI), laser-induced fluorescence excitation (LIF), resonant ion-dip infrared spectroscopy (RIDIRS), fluorescence-dip infrared spectroscopy (FDIRS), and UV−UV hole-burning spectroscopy, the conformational preferences of melatonin in a molecular beam have been determined. Three major *trans*-amide conformers and two minor *cis*-amide conformers have been identified in the R2PI spectrum and characterized with RIDIRS and FDIRS. Structural assignments are made using the infrared spectra in concert with density functional theory and localized MP2 calculations. Observation of *cis*-amide melatonin conformers in the molecular beam, despite the large energy gap (∼3 kcal/mol) between *trans*- and *cis*-amides, is striking because there are at least nine lower-energy *trans*-amide minima that are not detected. The implications of this observation for cooling and trapping conformational population in a supersonic expansion are discussed.

I. Introduction

Most molecules with biological relevance possess many flexible degrees of freedom, which produce a highly corrugated potential energy surface with several conformational minima. Often, these molecules adopt only one or a few preferred conformations, even though many structural possibilities exist. Understanding why a molecule adopts a specific conformation involves understanding the balance of forces that exist within the molecule and between that molecule and its surroundings. This is particularly important in small, biologically active molecules whose functions arise from their ability to dock in a receptor site and bind via noncovalent interactions such as hydrogen bonds. Ultimately, one would like to fully understand the conformational preferences and biological function of molecules in their native environments. Unfortunately, a molecular-scale understanding under physiological conditions is often hampered by the coexistence of several conformational isomers, the difficulty in assessing solvent effects, and the potential for rapid interconversion between conformational minima.

The study of such molecules in the gas phase removes solvent effects, thereby enabling the effects of intramolecular interactions to be assessed. The combination of double-resonance laser spectroscopy with supersonic expansion cooling provides a means of interrogating and structurally characterizing individual conformations of the flexible molecule, free from interference from other conformers and solvent effects.[1] One of the goals of experimental work on isolated, flexible biomolecules is to determine the preferred conformations and their relative conformer populations to benchmark calculations. In comparing experimental results with calculations, it is important to understand the relationship between the observed populations downstream in the expansion and the prenozzle Boltzmann distribution. In many cases, only conformations with relative energies within about 1 kcal/mol ($\sim kT_{\mathrm{nozzle}}$) of the global minimum are observed in the expansion.[1−7] In cases involving only a single torsional degree of freedom, simple rules have been developed regarding the height of the barrier needed to trap population behind it during supersonic expansion (∼400 cm^{-1}).[8] More recent studies on complex molecules with multiple degrees of conformational flexibility show that the barrier height needed to trap population in the expansion is closer to 1000 cm^{-1}.[9,10] As the number of conformational degrees of freedom grows, the relative populations observed after supersonic expansion will depend on the characteristics of the potential energy surface (i.e., the relative energies of minima, the

* Corresponding author. E-mail: zwier@purdue.edu. Phone: (765) 494-5278. Fax:(765) 494-0239.
[†] Purdue University.
[‡] University of Pittsburgh.

(1) Zwier, T. S. *J. Phys. Chem. A* **2001**, *105*, 8827.
(2) Carney, J. R.; Zwier, T. S. *J. Phys. Chem. A* **2000**, *104*, 8677.
(3) Carney, J. R.; Zwier, T. S. *Chem. Phys. Lett.* **2001**, *341*, 77.
(4) Robertson, E. G. *Chem. Phys. Lett.* **2000**, *325*, 299.
(5) Snoek, L. C.; Kroemer, R. T.; Hockridge, M. R.; Simons, J. P. *Phys. Chem. Chem. Phys.* **2001**, *3*, 1819.
(6) Unamuno, I. F.; Fernandez, J. A.; Longarte, A.; Castaño, F. *J. Phys. Chem. A* **2000**, *104*, 4364.
(7) Robertson, E. G.; Simons, J. P. *Phys. Chem. Chem. Phys.* **2001**, *3*, 1.
(8) Ruoff, R. S.; Klots, T. D.; Emilsson, T.; Gutowsky, H. S. *J. Chem. Phys.* **1990**, *93*, 3142.
(9) Godfrey, P. D.; Brown, R. D.; Rodgers, F. M. *J. Mol. Struct.* **1996**, *376*, 65.
(10) Godfrey, P. D.; Brown, R. D. *J. Am. Chem. Soc.* **1998**, *120*, 10724.

10.1021/ja0265916 CCC: $22.00

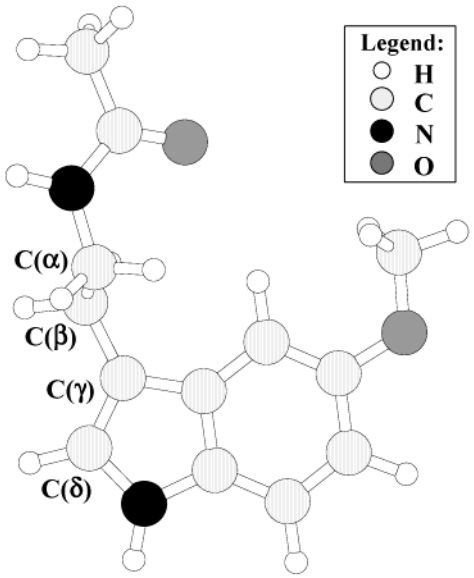

Figure 1. A picture of the melatonin molecule with the atom code and the important dihedral angles specified.

important pathways for conformational isomerization, and the heights of barriers separating them) and on the dynamics of cooling on that surface.

Melatonin (*N*-acetyl-5-methoxytryptamine, shown in Figure 1) contains a single methyl-capped amide group. As in peptides, there is a strong energetic preference in melatonin for *trans*-amide over *cis*-amide conformations, with the former about 3 kcal/mol more stable than the latter. Despite this fact, we shall see that it is possible to trap a small amount of the preexpansion population in the energetically unfavorable *cis*-amide branch because of the large barrier to *cis/trans* isomerization (∼15−20 kcal/mol).[11−13] Unlike many biomolecules that exist as zwitterions (e.g., the amino acids), melatonin has no significantly ionizable groups under physiological conditions, making the study of the conformational preferences of the neutral molecule directly relevant to its biological function.

In humans and other animal species, melatonin is a hormone that is primarily produced in the pineal gland, in small quantities in the retina, and in other tissues, with highest levels produced during the night.[14] Melatonin acts by specific binding to membrane receptors located in various regions of the brain and plays an important role as a transmitter of photoperiodic information, regulation of circadian rhythms and seasonal reproductive cycles, and mediation of other neuroendocrine and physiological processes.[15]

To date, the most sophisticated studies of the conformational preferences of melatonin have been experiments on the structure-affinity relationships (SARs) of melatonin and conformationally restricted melatonin analogues with natural membrane receptor tissues.[14] Several groups have used the SARs along with computational conformational searching to construct receptor[16,17] and pharmacophore models.[16,18] These studies indicate that both the methoxy and *N*-acetyl groups play an important role in the binding of melatonin with the native receptors, while the indole ring acts mainly as a spacer group, and the indole NH is not essential for activity.[14]

The work presented here addresses the conformational preferences of the isolated melatonin molecule, building on previous and ongoing studies of jet-cooled conformationally flexible biomolecules, such as neurotransmitters,[4,19] amino acids[5,9] and amino acid derivatives—histamine,[10] tryptamine,[1−3] 3-indolepropionic acid,[1,3] *N*-acetyl-tryptophan methyl amide,[20] *N*-acetyl-tryptophan ethyl ester,[20,21] and *N*-acetyl-tryptophan amide.[20,22]

II. Methods

A. Experimental. The experimental methods used in this study have been recently reviewed.[1] Melatonin was obtained commercially (97% pure, Sigma) and used without further purification. Jet-cooled melatonin was prepared by flowing either pure helium or a 70% neon/30% helium mixture at a backing pressure of 2−3 bar over the solid sample, heated to 470 K. This mixture was pulsed into the vacuum chamber at 20 Hz, using a high-temperature pulsed valve (General, Series 9, 0.8-mm diam). For interrogation by resonant two-photon ionization (R2PI), the expansion is skimmed ∼3 cm downstream from the nozzle orifice and mass-analyzed by time-of-flight mass spectrometry. Alternatively, the molecule was studied by laser-induced fluorescence following expansion in a free jet. In that case, the expansion is crossed with the UV excitation laser ∼4 mm downstream from the nozzle orifice, and the fluorescence is collected with an *f*:1 lens and imaged onto a UV-enhanced photomultiplier tube.

This work employs spectroscopic methods that are based on mass-selected two-color R2PI spectroscopy and LIF excitation spectroscopy. To obtain the two-color R2PI (2C-R2PI) spectrum of jet-cooled MEL, the doubled output of a Nd:YAG-pumped dye laser operating at 20 Hz was used to probe the $S_1 \leftarrow S_0$ transition. Typical unfocused UV output is 200 μJ/pulse using Rhodamine 640 (oscillator) and Rhodamine 610 (amplifier), both in ethanol, Sulforhodamine 640 in methanol, or DCM in methanol. The third harmonic of a Nd:YAG laser (355 nm) was used for the ionization step, $D_0 \leftarrow S_1$. Typical 355-nm power was 1 mJ/pulse. The 355-nm laser was spatially and temporally overlapped with the UV laser. Cannington and Ham report the vertical ionization potential of melatonin as 7.7 eV, with an approximate value of 7.03 eV for the adiabatic ionization threshold.[23]Using the latter value (56697 cm^{-1}) as the ionization potential, 2C-R2PI through the melatonin S_1-S_0 origin reaches 4000 cm^{-1} above the ionization threshold, compared to about 8500 cm^{-1} in the one-color R2PI scheme. 2C-R2PI was used instead of 1C-R2PI because unsaturated R2PI spectra could be obtained with enhanced ionization efficiency and no detectable fragmentation.

In the flexible molecules, mass analysis cannot be used to separate the various conformational isomers present in the R2PI spectrum. The double-resonance technique of UV−UV hole-burning spectroscopy was used to obtain R2PI spectra of individual conformational isomers, free from interference from one another. The UV−UV hole-burning spectra were obtained by fixing the hole-burning UV laser (10 Hz) on the origin transition of a particular conformer and tuning a time-delayed probe

(11) Scherer, G.; Kramer, M. L.; Schutkowski, M.; Reimer, U.; Fischer, G. *J. Am. Chem. Soc.* **1998**, *120*, 5568.
(12) Schiene-Fischer, C.; Fischer, G. *J. Am. Chem. Soc.* **2001**, *123*, 6227.
(13) Li, P.; Chen, X. G.; Shulin, E.; Asher, S. A. *J. Am. Chem. Soc.* **1997**, *119*, 1116.
(14) Mor, M.; Plazzi, P. V.; Spadoni, G.; Tarzia, G. *Curr. Med. Chem.* **1999**, *6*, 501.
(15) Reiter, R. J. *Endocrine Rev.* **1991**, *12*, 151.
(16) Jansen, J. M.; Copinga, S.; Gruppen, G.; Molinari, E. J.; Dubocovich, M. L.; Grol, C. J. *Bioorganic Med. Chem.* **1996**, 1321.
(17) Grol, C. J.; Jansen, J. M. *Bioorg. Med. Chem.* **1996**, *4*, 1333.
(18) Sicsic, S.; Serraz, I.; Andrieux, J.; Bremont, B.; Mathe-Allainmat, M.; Poncet, A.; Shen, S.; Langlois, M. *J. Med. Chem.* **1997**, *40*, 739.
(19) Butz, P.; Kroemer, R. T.; Macleod, N. A.; Simons, J. P. *J. Phys. Chem. A* **2001**, *105*, 544.
(20) (a) Dian, B. C.; Longarte, A.; Mercier, S.; Zwier, T. S. In preparation. (b) Dian, B. C.; Longarte, A.; Zwier, T. S. *Science* **2002**, *296*, 2369.
(21) Park, Y. D.; Rizzo, T. R.; Peteanu, L. A.; Levy, D. H. *J. Chem. Phys.* **1986**, *84*, 6539.
(22) Tubergen, M. J.; Cable, J. R.; Levy, D. H. *J. Chem. Phys.* **1990**, *92*, 51.
(23) Cannington, P. H.; Ham, N. S. *J. Electron Spectrosc. Relat. Phenom.* **1983**, *32*, 139.

UV laser (20 Hz) through the R2PI spectrum, while monitoring the difference in ion current with and without the hole-burning laser present. All of the vibronic transitions that arise from the same ground-state level as the hole-burned origin transition show up as depletions in the hole-burning spectrum.

Infrared spectra in the hydride-stretch region of individual melatonin conformers are obtained using a second double-resonance technique, known as resonant ion-dip infrared spectroscopy (RIDIRS).[1] For such scans, the infrared output (2200−4000 cm^{-1}) of an injection seeded Nd:YAG-pumped optical parametric converter was spatially overlapped with the two R2PI lasers, preceding them by 50−200 ns. 2C-R2PI, with λ_1 fixed to a given conformer $S_1 \leftarrow S_0$ origin, generates a constant ion signal in the melatonin monomer mass channel because of a single conformation of melatonin. The IR laser is operated at 10 Hz and tuned through the hydride-stretching region, depleting population out of the ground vibrational level whenever it is resonant with a vibration in the monomer of interest. Using active baseline subtraction, infrared transitions in the ground-state monomer conformation are thus detected as depletions in the ion current.

For melatonin conformers with very small populations in the expansion, we utilized the fluorescence-based analogue of RIDIRS (namely, fluorescence-dip infrared spectroscopy or FDIRS) to obtain infrared spectra. For FDIRS, a free-jet expansion of melatonin in helium was crossed 4 mm downstream by the counterpropagating IR and UV lasers. The laser-induced fluorescence of a specific conformer is monitored, while the IR source is tuned throughout the hydride-stretching region, just as in RIDIRS. While mass resolution is lost using the LIF-based method, the increase in signal to noise provided superior spectra of the smaller conformers using LIF detection.

B. Computational. To screen potential conformations adopted by flexible molecules such as melatonin, it is useful to run computationally inexpensive molecular mechanics conformational searches. Although the use of molecular mechanics methods such as AMBER, OPLS, MM3, and CHARMM to determine the relative conformational energies of gas phase molecules is not quantitatively accurate,[24] these methods are efficient for generating reasonable starting structures for quantum mechanical calculations. Conformational searching on melatonin was performed within MacroModel version 7.1[25] using the OPLS-AA force field[26] and the Monte Carlo search protocol. The OPLS-AA force field has been tested for accuracy in isolated molecule conformational energetics and found to be among the best force fields for this purpose.[24] All dihedral angles of the melatonin flexible side chain and methoxy group were allowed to vary, with the exception of the methyl rotors, which were held in optimized geometries. An energy cutoff of 12 kcal/mol was used in the conformational searching.

The lowest energy structures (those within ~5 kcal/mol of the lowest energy structure) generated by the OPLS-AA conformational search served as starting structures for full optimization via ab initio or density functional theory methods using the Gaussian 98 suite of programs.[27] The Hartree−Fock (HF) method was used for a second-level screening, with the lowest 12 energy HF *trans*-amide minima, along with six *cis*-amide structures, being optimized using density functional theory calculations using the Becke3LYP functional.[29,30] Harmonic vibrational frequencies and infrared intensities were also computed for comparison with the experimental infrared spectra. All of these calculations employed the 6-31+G*(5d) basis set.[28]

Finally, localized MP2/aug-cc-pVTZ(-f) single-point energy calculations were performed on eight of the most relevant MEL structures (four *trans*/anti, three *trans*/syn, and one *cis*/anti) to assess the accuracy of the relative energies obtained with the Becke3LYP method. The two main drawbacks of the B3LYP/6-31+G*(5d) procedure for predicting the relative energies of conformers of molecules such as melatonin are its failure to describe long-range dispersion interactions and its sizable basis set superposition errors (BSSE).[31] The adoption of the LMP2[32,33]/aug-cc-pVTZ(-f)[34−36] approach addresses both of these issues, properly describing dispersion interactions, while minimizing the effects of BSSE. The basis set employed is that of Dunning et al.,[34−36] but with the f-functions and d-functions removed from the heavy elements and hydrogen atoms, respectively. Both the adoption of the LMP2 procedure and the flexible aug-cc-pVTZ(-f) basis set are important for minimizing the BSSE. In the LMP2 method, the canonical HF orbitals are localized, and the excitation space used to correlate the localized occupied orbitals is restricted to atomic functions centered upon these atoms. The LMP2 algorithm used in this study is the pseudospectral implementation of Murphy et al.[37] and included in the Jaguar[38] suite of programs. The Pipek−Mezey[39] procedure for orbital localization was used. LMP2 energies were calculated at the B3LYP/6-31+G*(5d) optimized geometries. Test calculations on the related tryptamine molecule show that the errors in the relative energies because of the use of the Becke3LYP geometries are quite small, and the same is expected to be true for melatonin.

III. Results and Analysis

A. Calculated Structures, Energetics, and Vibrational Frequencies of the Conformers. While there have been previous computational studies focused on the conformational preferences of melatonin, these calculations were carried out using AM1,[40] MM2*,[16] and MM3[41] force fields or the HF method with minimal basis sets.[40,41] We therefore sought to carry out a more complete conformational search and to substantially improve the quantitative predictions of relative conformational energy using the procedure outlined in Section II. B. By combining force field searching with electronic structure calculations, we have generated a more reliable set of structures with predictions for the infrared spectra that can aid our spectral assignments.

The OPLS-AA conformational searching yielded 204 unique minima within 12 kcal/mol of the global minimum. These conformers fall into one of four families: *trans*/anti, *trans*/syn, *cis*/anti, and *cis*/syn, where *trans* (*cis*) refers to the structure of the amide group and anti (syn) refers to the orientation of the

(24) Beachy, M. D.; Chasman, D.; Murphy, R. B.; Halgren, T. A.; Friesner, R. A. *J. Am. Chem. Soc.* **1997**, *119*, 5908.
(25) Mohamadi, F.; Richard, N. G. J.; Guida, W. C.; Liskamp, R.; Lipton, M.; Caufield, C.; Chang, G.; Hendrickson, T.; Still, W. C. *J. Comput. Chem.* **1990**, *11*, 440.
(26) Jorgensen, W. L.; Maxwell, D. S.; Tirado-Rives, J. *J. Am. Chem. Soc.* **1996**, *118*, 11225.
(27) Frisch, M. J.; Trucks, G. W.; Schlegel, H. B.; Scuseria, G. E.; Robb, M. A.; Cheeseman, J. R.; Zakrzewski, V. G.; Montgomery, J. A.; Stratmann, R. E.; Burant, J. C.; Dapprich, S.; Millam, J. M.; Daniels, A. D.; Kudin, K. N.; Strain, M. C.; Farkas, O.; Tomasi, J.; Barone, V.; Cossi, M.; Cammi, R.; Mennucci, B.; Pomelli, C.; Adamo, C.; Clifford, S.; Ochterski, J.; Petersson, G. A.; Ayala, P. Y.; Cui, Q.; Morokuma, K.; Malick, D. K.; Rabuck, A. D.; Raghavachari, K.; Foresman, J. B.; Cioslowski, J.; Ortiz, J. V.; Baboul, A. G.; Stefanov, B. B.; Liu, G.; Liashenko, A.; Piskorz, P.; Komaromi, I.; Gomperts, R.; Martin, R. L.; Fox, D. J.; Keith, T.; Al-Laham, M. A.; Peng, C. Y.; Nanayakkara, A.; Gonzalez, C.; Challacombe, M.; Gill, P. M. W.; Johnson, B.; Chen, W.; Wong, M. W.; Andres, J. L.; Gonzalez, C.; Head-Gordon, M.; Replogle, E. S.; Pople, J. A. *Gaussian 98*; Gaussian, Inc.: Pittsburgh, PA, 1998.
(28) Frisch, M. J.; Pople, J. A.; Binkley, J. S. *J. Chem. Phys.* **1984**, *80*, 3265.
(29) Becke, A. D. *J. Chem. Phys.* **1993**, *98*, 5648.
(30) Lee, C.; Yang, W.; Parr, R. G. *Phys. Rev. B* **1988**, *37*, 785.
(31) Boys, S. F.; Bernardi, F. *Mol. Phys.* **1970**, *19*, 553.
(32) Sæbø, S.; Pulay, P. *Theor. Chim. Acta* **1986**, *69*, 357.
(33) Sæbø, S.; Pulay, P. *Ann. Phys. Rev. Chem.* **1993**, *44*, 213.
(34) Dunning, T. H. *J. Chem. Phys.* **1989**, *90*, 1007.
(35) Kendall, R. H.; Dunning, T. H.; Harrison, R. J. *J. Chem. Phys.* **1992**, *96*, 6796.
(36) Woon, D. E.; Dunning, T. H., Jr. *J. Chem. Phys.* **1993**, *98*, 1358.
(37) Murphy, R. B.; Beachy, M. D.; Friesner, R. A.; Ringnalda, M. N. *J. Chem. Phys.* **1995**, *103*, 1481.
(38) *Jaguar*; Schrödinger, Inc: Portland, 1991−2000.
(39) Pipek, J.; Mezey, P. G. *J. Chem. Phys.* **1989**, *90*, 4916.
(40) Vasilescu, D.; Broch, H. *J. Mol. Struct. (THEOCHEM)* **1999**, *460*, 191.
(41) Lopez Sastre, J. A.; Miguel, R. N.; Molina, R. P.; Zarzuelo, M. C. G.; Romero-Avila, C.; Ramos, A. G. *J. Mol. Struct. (THEOCHEM)* **2001**, *537*, 271.

Table 1. Relative Energies of a Selection of MEL Conformational Minima[a]

MEL Conformer	ΔE (B3LYP)	ΔE (B3LYP+ZPE)	ΔE (LMP2)	ΔE (LMP2+ZPE)
Anti(*trans*-out)/anti	0.00[b]	0.00[c]	0.00[d]	0.00[c]
Gpy(*trans*-in)/anti	0.28	0.30	0.56	0.58
Gph(*trans*-in)/anti	0.68	0.69	0.71	0.72
Anti(*trans*-in)/anti	0.88	0.77	1.62	1.50
Gpy(*trans*-in)/syn	1.14	1.12	3.02	3.00
Gph(*trans*-in)/syn	1.54	1.54	3.07	3.08
Anti(*trans*-out)/syn	2.04	1.94	3.56	3.46
Gph(*cis*-in)/anti	2.70	2.92	2.36	2.58

[a] The energies are calculated via Becke3LYP/6-31+G*(5d) full geometry optimizations and single-point localized MP2/aug-cc-pVTZ(-f) calculations. Zero-point energy contributions are determined at the Becke3LYP/6-31+G*(5d) level of theory. [b] The absolute energy of Anti(*trans*-out)/anti is −480106.3125 kcal/mol (DFT). [c] The zero-point energy of Anti(*trans*-out)/anti is 172.2339 kcal/mol (DFT). [d] The absolute energy of Anti(*trans*-out)/anti is −478956.1835 kcal/mol (LMP2).

methoxy group with respect to the indole NH. Approximately 40 of the lowest energy OPLS-AA structures were further optimized using the HF/6-31+G*(5d) method. The energy ordering of the HF optimized structures differs significantly from the OPLS-AA calculations. Becke3LYP/6-31+G*(5d) geometry optimizations and harmonic frequency calculations were performed on the twelve lowest energy structures obtained from the HF calculations (all *trans*-amides), along with six higher energy *cis*-amide structures. The energy ordering of the DFT optimized MEL conformers, both zero-point energy uncorrected and corrected, agrees well with the HF calculations. Finally, single-point LMP2/aug-cc-pVTZ(-f) calculations were performed on eight of the lowest-energy conformers, including four *trans*/anti, three *trans*/syn, and one *cis*/anti structures. Table 1 summarizes the relative energies obtained using both the DFT and LMP2 methods. While the LMP2 method predicts the same ordering of the four lowest energy minima as the DFT method, the relative energies of the various families changes significantly between DFT and LMP2. In the table, the zero-point energy corrections for the LMP2 results are obtained from the DFT harmonic frequencies.

Select DFT optimized structures are shown pictorially in Figure 2. In all calculated structures, the oxygen and carbon atoms of the methoxy group lie in the plane of the indole ring. The lowest energy conformations of MEL have the methoxy group pointed anti with respect to the indole NH, regardless of the orientation of the amide group and the position of the backbone. Not surprisingly, the lowest energy DFT calculated conformations of MEL have the amide group in a trans configuration. Almost all of the low-energy structures of MEL have the C(α)−C(*β*) bond nearly perpendicular to the ring. The *N*-acetyl group then takes up various positions relative to the indole ring: anti, gauche toward the pyrrole ring (Gpy), and gauche toward the phenyl ring (Gph) of indole. This is the same nomenclature used to denote the position of the ethylamine or propionic acid side chains in TRA and IPA.[1−3] In addition, MEL has flexibility associated with the orientation of the *N*-acetyl and methoxy groups. Thus, the four lowest energy structures are denoted Anti(*trans*-out)/anti, Gpy(*trans*-in)/anti, Gph(*trans*-in)/anti, and Anti(*trans*-in)/anti, where the notation is defined as backbone position(amide NH orientation)/methoxy position and "in" or "out" refers to whether the amide NH is pointed in toward or out away from the indole ring.

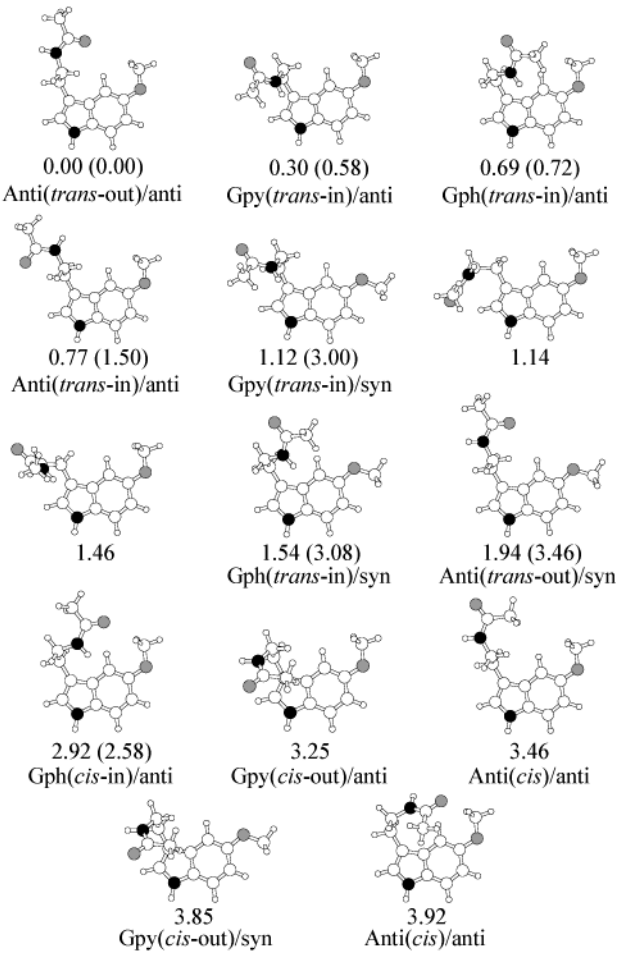

Figure 2. A summary of selected conformational minima of MEL obtained via Becke3LYP/6-31+G*(5d) calculations. The DFT zero-point corrected relative energies in kcal/mol are displayed beneath each structure, and where available, the localized MP2/aug-cc-pVTZ(-f) relative energies are shown in parentheses. Minima are observed for the four families of MEL with the energy ordering: *trans*-amide/anti-methoxy < *trans*/syn < *cis*/anti < *cis*/syn.

The structures in Figure 2 depict nine of the lowest energy *trans*-amide structures, and the lowest five *cis*-amide structures with their energies listed relative to the global minimum determined by the DFT method. The zero-point corrected LMP2 energies are also given for select conformations in parentheses. According to the DFT calculations, the four most stable structures are all within 1 kcal/mol of one another. The Anti-(*trans*-out)/anti structure is the global minimum, and the Gpy(*trans*-in)/anti and Gph(*trans*-in)/anti structures are slightly higher in energy at 0.30 and 0.69 kcal/mol, respectively. The next highest energy structure, at 0.77 kcal/mol, is a second Anti *N*-acetyl structure labeled Anti(*trans*-in)/anti, which differs from the global minimum primarily by rotation about the C(α)−N(H) bond.

The LMP2/aug-cc-pVTZ(-f) single-point energy calculations retain the Anti(*trans*-out)/anti structure as the global minimum but raise the energy of the other *trans*/anti minima relative to it. The relative energy of the fourth minimum (Anti(*trans*-out)/anti) is affected most noticeably by the level of theory, being pushed up from 0.77 to 1.50 kcal/mol, including zero-point energy correction. Thus, the LMP2 calculations predict that three structures, Anti(*trans*-out)/anti, Gpy(*trans*-in)/

anti, and Gph(*trans*-in)/anti, are at least 0.8 kcal/mol more stable than all other structures.

The energetically preferred position for the methoxy group is "anti" over "syn". In the DFT calculations, the Gpy(*trans*-in)/syn, Gph(*trans*-in)/syn, and Anti(*trans*-out)/syn minima are located 1.12, 1.54, and 2.04 kcal/mol, respectively, above the global minimum. This preference for anti over syn methoxy structures is predicted to be even greater by the LMP2 calculations. The energies of the Gpy(*trans*-in)/syn, Gph(*trans*-in)/syn, and Anti(*trans*-out)/syn minima are raised to 3.00, 3.08, and 3.46 kcal/mol, respectively, above the global minimum. This would seem to suggest that dispersion interactions are more significant in the MEL conformations with a syn-oriented methoxy group.

The lowest energy *cis*-amide MEL conformers are also approximately 3 kcal/mol higher in energy than the Anti(*trans*-out)/anti global minimum. The lowest energy *cis*-amide MEL conformer is the Gph(*cis*-in)/anti structure at 2.92 (2.58) kcal/mol above the global minimum using DFT (LMP2) (Figure 2). The calculated *cis*-amide MEL minima show a greater variability in the degree of rotation about the C(α)−C(β) bond than the corresponding *trans*-amide minima.

Hydride stretch harmonic vibrational frequencies and infrared intensities calculated at the DFT Becke3LYP/6-31+G*(5d) level of theory are summarized for the relevant conformers in the Supporting Information. A scale factor of 0.96 has been used to align the calculated frequency of the indole NH to its experimental value. Unfortunately, this same scale factor overestimates the CH stretch frequencies by about 60 cm^{-1}.

The frequency of the amide NH stretch fundamental is most sensitive to the MEL conformation, suggesting that this band will play a key role in the comparison between experiment and theory in making conformational assignments. For *trans*-amide MEL conformers, the amide NH stretch appears either as a free NH stretch (3495 cm^{-1}) or slightly shifted down in frequency because of a weak interaction of the NH group with the π cloud of indole. By comparison, all *cis*-amide MEL conformers have an amide NH stretch that is lowered in frequency by about 50 cm^{-1} relative to their *trans*-amide counterparts. This shift can serve as a marker to distinguish *cis*-amide from *trans*-amide structures. The hydride stretch vibrational frequencies also encompass a range of CH stretch vibrations because of aromatic (3000−3100 cm^{-1}), CH_2, and CH_3 groups. The strong methoxy symmetric stretch vibration (~2900 cm^{-1}) shows little dependence on the methoxy orientation (syn or anti), and thus is not anticipated to be an effective means of discriminating between these structures.

B. LIF, R2PI, and UV−UV Hole-Burning Spectroscopy. A portion of the LIF excitation spectrum of MEL in a helium expansion is shown in Figure 3. The LIF spectrum is dominated by two transitions labeled A (32614 cm^{-1}) and B (32621 cm^{-1}). Several less intense transitions are observed both to the red and blue of these transitions. The transitions labeled C (32795 cm^{-1}), D (32483 cm^{-1}), and E (32432 cm^{-1}) have intensities 17%, 5%, and 0.8% of transition A, respectively. The transition just to the blue of E, which is marked with an asterisk, is due to a MEL−(H_2O) complex, as determined by mass analysis and infrared spectroscopy, and will be discussed in a forthcoming paper.[42]

(42) Florio, G. M.; Zwier, T. S. In preparation.

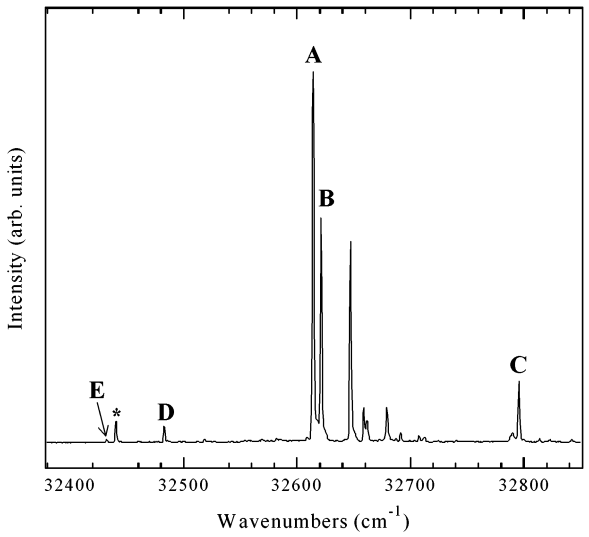

Figure 3. A portion of the LIF spectrum of MEL. The letters indicate the five distinct melatonin conformer $S_1 \leftarrow S_0$ origin transitions. The asterisk designates a MEL−W_1 cluster observed in the LIF spectrum at 32441 cm^{-1}.

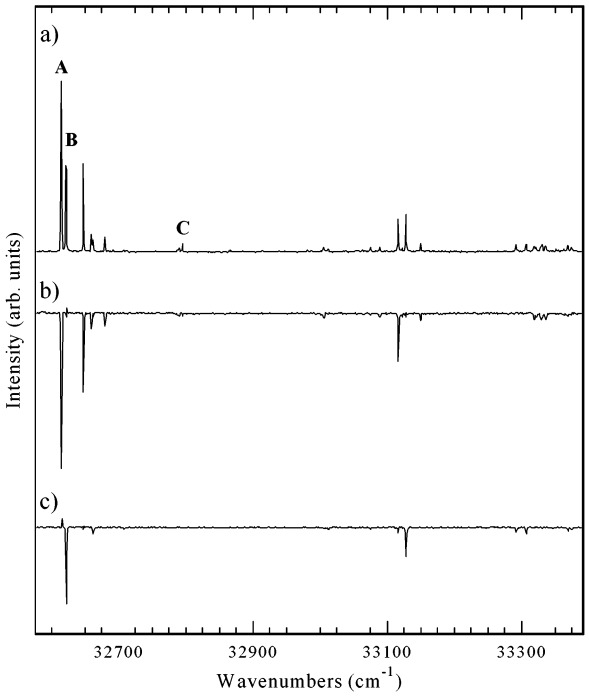

Figure 4. (a) 2C-R2PI spectrum taken in the MEL^+ mass channel (m/z = 232) and (b,c) UV−UV hole-burning spectroscopy with the hole-burning laser fixed on the S_1-S_0 origin transition of (b) MEL A (32614 cm^{-1}) and (c) MEL B (32621 cm^{-1}). The hole-burning spectra indicate that MEL A and B are distinct origin transitions arising from different MEL conformations. All of the vibronic structure observed in the R2PI spectrum is cleanly divided between the A and B conformers, with the exception of the transition labeled C (32795 cm^{-1}). See text for further discussion.

We anticipate that the LIF spectrum of Figure 3 contains overlapping spectra because of different conformational isomers of MEL. To determine the number of conformations present and to identify their ultraviolet spectra, UV−UV hole-burning spectroscopy is used, here on the basis of 2C-R2PI detection. Figure 4a presents the 2C-R2PI spectrum (λ_{ion} = 355 nm) for comparison with the hole-burning spectra of Figure 4b and 4c, all recorded in the MEL monomer mass channel (m/z = 232). These spectra were taken with a 70% neon/30% helium expansion mixture. The hole-burning laser was fixed on the

transitions labeled A in recording Figure 4b and transition B to record Figure 4c. The hole-burning spectra prove that A and B are two distinct MEL species and therefore represent different conformational isomers. All of the transitions to the blue of A and B belong to one of these two conformers, with the exception of transition C, which will be discussed separately below.

The hole-burning spectra of Figure 4b and 4c provide the ultraviolet spectra of the two dominant MEL conformers, free from interference from one another. These two conformers are hereafter denoted A and B, respectively, in keeping with their origin transition labels. The R2PI spectra for MEL A (Figure 4b) and MEL B (Figure 4c**)** bear a close resemblance to one other and are characteristic of the ultraviolet spectra of indole[43] and other indole derivatives.[2,43] Both MEL conformers undergo only small changes in geometry upon electronic excitation, with intense origin transitions and relatively weak vibronic structure. For both MEL A and B, a progression in a low-frequency vibrational mode (33 cm^{-1} for A, 41 cm^{-1} in B) is observed, built off the origin transitions and off a vibronic band at +500 cm^{-1}. The nature of this low-frequency vibration is one that involves motion of the MEL side chain with respect to the indole ring. A likely candidate is the butterfly motion at ~30 cm^{-1} in the DFT calculations. The greater intensity of this low-frequency progression in A than B suggests a stronger interaction of the side chain with the π cloud in the former over the latter.

On the basis of a comparison with the DFT calculations, the vibronic transitions at approximately 500 cm^{-1} above both A and B are assigned to a C−C/C═C vibration involving expansion of the indole ring, consistent with the expected change in the ring induced by the $\pi-\pi^*$ transition. Not surprisingly, this +500 cm^{-1} vibration is observed in the R2PI spectra of most other indole derivatives.[2,43−46] The frequencies of the vibronic transitions for each conformer and their relative intensities are summarized in Table 2.

As mentioned earlier, the only transition in the portion of the R2PI spectrum shown in Figure 4a that is not a vibronic band of MEL A or B is the transition labeled C at 32795 cm^{-1}. Because this transition does not burn out with either MEL A or B, we know that the carrier of this transition is a species distinct from A and B. The infrared spectrum recorded when monitoring transition C (Section C) will provide further proof that this transition is due to a third MEL conformation. The intensity of the MEL C origin (relative to A and B) in the LIF spectrum taken in a helium expansion (Figure 3) is considerably greater than its intensity in the 2C-R2PI spectrum taken in a 70% neon/30% helium expansion (Figure 4a). An LIF spectrum using 70% neon/30% helium confirms that it is the difference in expansion conditions, rather than any difference in detection efficiency in LIF versus R2PI, that is responsible for the observed intensity change. The sensitivity of the population of conformer C to the presence of neon in the expansion indicates that the barrier to isomerization out of minimum C must be small enough that collisional cooling can effect this population.[9,10] On the basis of the relative intensities of A, B, and C under both expansion conditions, it appears that the population from conformer C is being funneled into conformer A in the neon expansion.

The UV−UV hole-burning spectra of MEL D and E (Figure 3) were not obtained because the transitions are weak enough that it was difficult to see the vibronic structure among the much more intense bands because of A and B. Coincidentally, the MEL D transition occurs at the same frequency as a vibronic transition of a MEL−$(water)_1$ cluster appearing in the MEL−$(water)_1^+$ mass channel.[42] To determine that the carrier of this band in the MEL^+ mass channel was a monomer species and not a water cluster, a 1C-R2PI spectrum was recorded in the absence of water flow in the expansion (not shown). The MEL D and E transitions are retained in the absence of water flow at the same intensity relative to A and B, while the transition in the MEL−$(water)_1^+$ mass channel disappears. Most importantly, the FDIR spectra of the D and E transitions reveal that they are in fact additional monomer species, unique from each other and from the MEL A, B, and C conformers. The MEL D and E transitions are not affected by expansion conditions.

It is concluded that the transitions labeled A−E are the $S_1 \leftarrow S_0$ origin transitions of five distinct MEL conformers. R2PI spectra extending 600 cm^{-1} below the E transition reveal no further monomer structure. The MEL A, B, C, D, and E origin transitions at 32614, 32621, 32795, 32483, and 32432 cm^{-1}, respectively, are $\pi-\pi^*$ excitations of the indole moiety and are shifted 2400−2800 cm^{-1} to the red of the indole origin at 35239 cm^{-1}.[43] For comparison, the $S_1 \leftarrow S_0$ origin transitions of 3-methylindole, tryptamine conformer A, and 5-methoxyindole are shifted to the red of the indole origin by 362 cm^{-1},[43] 320 cm^{-1},[2] and 2103 cm^{-1},[43] respectively. Thus, it is the presence of the methoxy group at the C5 position that is responsible for the dramatic stabilization of the excited electronic state of melatonin with respect to that of indole.

As Figure 3 shows clearly, the $S_1 \leftarrow S_0$ origin transitions of the five conformers naturally break up into the A/B pair near 32600 cm^{-1}, the D/E pair near 32400 cm^{-1}, and the lone transition C near 32800 cm^{-1}. This natural grouping of transition frequencies suggests a similar structural grouping in the five conformers. However, the electronic frequency shift is a measure of the separation between S_0 and S_1 states and is difficult to correlate with distinct structural features of the individual conformations, which perturb the π cloud of indole via both through-space and through-bond interactions. Instead, we turn next to the infrared spectra, which can provide a more direct and sensitive probe of the conformations of MEL.

C. RIDIR and FDIR Spectroscopy. The RIDIR spectra of the MEL A and B conformers and the FDIR spectra of the MEL C−E conformers in the CH and NH stretching region (2800−3800 cm^{-1}) are shown in Figure 5a−e, respectively. Because of the weaker intensity of transitions C−E, their FDIR spectra were recorded with about a factor of 2 higher infrared intensity and hence are somewhat more saturated than the RIDIR spectra of A and B. The infrared spectra of the MEL conformers exhibit two NH stretch fundamentals in the 3400−3600 cm^{-1} region, and a collection of aromatic, alkyl, and methyl CH stretch fundamentals spread over the region from 2800 to 3100 cm^{-1}. In all five conformers, the indole NH stretch appears between 3522 and 3526 cm^{-1}, very close to its frequency in the indole monomer (3525 cm^{-1}).[45] Not surprisingly, this fundamental is not sensitive to the conformations of the side chains.

On the other hand, the amide NH stretch fundamental is much more sensitive to conformational change, varying between 3420

(43) Huang, Y.; Sulkes, M. *J. Phys. Chem.* **1996**, *100*, 16749.
(44) Carney, J. R.; Zwier, T. S. *J. Phys. Chem. A* **1999**, *103*, 9943.
(45) Carney, J. R.; Hagemeister, F. C.; Zwier, T. S. *J. Chem. Phys.* **1998**, *108*, 3379.
(46) Arnold, S.; Sulkes, M. *Chem. Phys. Lett.* **1992**, *200*, 125.

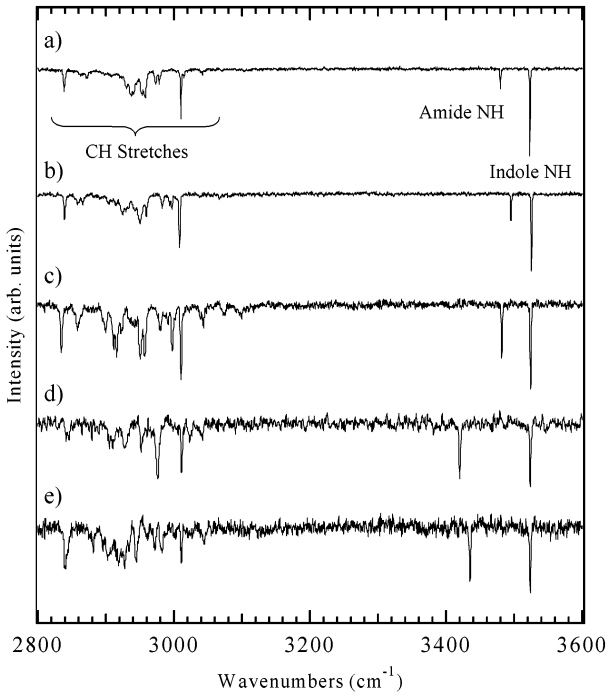

Figure 5. Overview of the RIDIR and FDIR spectra of the five MEL conformers taken with the UV laser fixed to the origin transitions of (a) MEL A, (b) MEL B, (c) MEL C, (d) MEL D, and (e) MEL E. The position of the indole NH stretch, the amide NH stretch, and the CH stretch region are specified.

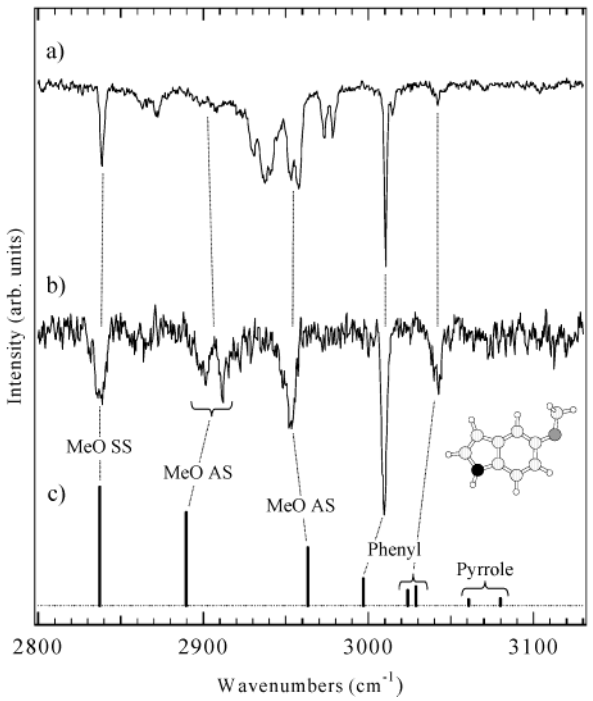

Figure 6. A comparison of the IR spectra of (a) MEL A, (b) 5-methoxyindole, and (c) the Becke3LYP/6-31+G*(5d) calculated harmonic IR spectrum of 5-methoxyindole in the CH stretching region. The frequencies in the calculated spectrum (c) have been scaled by 0.94, thereby aligning the calculated and experimental methoxy CH_3 symmetric stretching mode of 5-methoxyindole. Assignments of CH stretches between 5-methoxyindole and MEL A are shown by the dashed lines. See text for discussion.

and 3495 cm^{-1}. A first classification is obvious from Figure 5: while the amide NH stretch fundamentals of conformers A, B, and C appear at or above 3480 cm^{-1} (3480, 3495, and 3482 cm^{-1}, respectively), those due to D and E are shifted below 3440 cm^{-1} (specifically, at 3420 and 3435 cm^{-1}, respectively). Furthermore, the set of three high-frequency conformers break up further into a set of two (A and C at 3480 and 3482 cm^{-1}) and conformer B, with its highest frequency amide NH stretch at 3495 cm^{-1}.

The CH stretch region of the spectra is complicated by the sheer number of fundamentals because of aromatic CH, alkyl CH_2, methyl groups, and the potential for Fermi resonance with overtones of lower-frequency vibrations. The CH stretch region of each conformer is unique and can potentially serve as a confirming diagnostic of the molecular conformation. In particular, the CH stretches of the MEL A, B, and C share common features that are distinct from those of MEL D and E. This suggests that the MEL A, B, and C conformers have a structural similarity not shared by MEL D and E.

In an attempt to understand the complex CH stretch region of the MEL conformers, we have obtained the FDIR spectrum of 5-methoxyindole (5-MOI), which removes the transitions due to the side chain in the 3-position in MEL, thereby highlighting the CH stretch transitions due to the 5-methoxy methyl group and the indole ring. The FDIR spectrum of 5-methoxyindole is shown in Figure 6b and is compared both with the Becke3LYP/6-31+G*(5d) calculated harmonic infrared spectrum of 5-MOI (Figure 6c) and the MEL conformer A RIDIR spectrum (Figure 6a). On the basis of a comparison of the FDIR (Figure 6b) and calculated (Figure 6c) spectra of 5-MOI, all of the experimental transitions can be assigned. The methoxy methyl group produces three CH stretch fundamentals spread over the 2800−3000 cm^{-1} region. The symmetric methyl stretch occurs at 2837 cm^{-1}, while the two "antisymmetric" methyl CH stretch bands appear as a Fermi dyad at 2912/2902 and at 2952 cm^{-1}. The experimental spectrum contains only two other CH stretch bands (3010 and 3042 cm^{-1}), ascribable to the aromatic CH stretch fundamentals of the indole ring. The likely correspondence with the calculated aromatic fundamentals is made by the dashed lines in Figure 6. The weak bands above 3050 cm^{-1} are not clearly observed in the experimental spectra.

The FDIR spectrum of 5-MOI can then be used to identify the corresponding methoxy CH stretch bands in the MEL conformers, since the frequencies of the aromatic and methoxy CH stretches in the MEL A spectrum (Figure 6a) are essentially unaltered from their values in 5-MOI (Figure 6b). Analogous bands are apparent in MEL B−E as well. In particular, the dominant aromatic CH stretch band at 3010 cm^{-1} and the methoxy symmetric stretch at ∼2840 cm^{-1} are easily identifiable in all spectra. Only small changes are observed in this latter band (occurring at 2839 in MEL A, 2839 in MEL B, 2834 in MEL C, 2841 in MEL D, and 2839 cm^{-1} in MEL E), suggesting that all five conformers share the same methoxy group orientation as observed in 5-MOI. However, the calculations show almost no change in the methoxy methyl CH stretch frequencies with methoxy group orientation, making this vibration uninformative regarding a syn/anti assignment. By process of elimination, the remaining bands in the MEL A spectrum thus arise from the $CH_2(\alpha)$, $CH_2(\beta)$, and *N*-acetyl methyl CH stretching modes of the side chain. A comparison of the MEL CH stretch spectra with the $CH_2(\alpha)$ and $CH_2(\beta)$ transitions in tryptamine suggests that much of the observed transitions unaccounted for by the methoxy and indole CH stretches is due to the $CH_2(\alpha,\beta)$ groups.

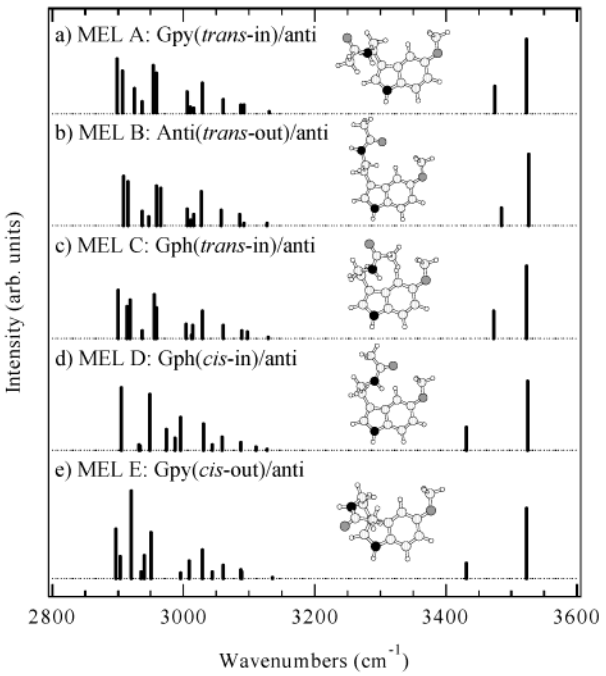

Figure 7. (a−e): Calculated harmonic vibrational frequencies and infrared intensities for the CH and NH stretch vibrations of the Gpy(*trans*-in)/anti, Anti(*trans*-out)/anti, Gph(*trans*-in)/anti, Gph(*cis*-in)/anti, and Gpy(*cis*-out)/anti conformers of MEL. The structures of these conformers are shown as insets. All calculated frequencies have been scaled by 0.96 to bring the calculated indole NH stretch frequency into coincidence with its experimental value (3525 cm^{-1}).

D. Conformational Assignments. As the results of Sections B and C indicate, the frequency of the amide NH stretch fundamental is anticipated to provide the clearest basis of distinction between the various MEL conformations, guided by the calculations. Figure 7 presents the harmonic infrared frequencies and infrared intensities of the lowest three *trans*-amide conformers (Figure 7a−c) and lowest two *cis*-amide conformers (Figure 7d, e) of MEL, calculated at the DFT Becke3LYP/6-31+G*(5d) level of theory. As noted previously, the calculations predict that the *cis*-amide NH stretch fundamentals are characteristically lower in frequency than their *trans*-amide counterparts by about 40−50 cm^{-1}. No other structural change (e.g., syn/anti methoxy or gauche/anti *N*-acetyl) is capable of producing a change in the amide NH stretch of this magnitude. Table 3 compares the experimental and calculated shift of the amide NH stretch frequency from the indole NH stretch for the lowest three *trans*-amide and lowest two *cis*-amide conformers. This shift serves as an excellent indicator of the orientation of the amide group, *trans* versus *cis*, and leads us to assign the dominant MEL A, B, and C conformers to *trans*-amide conformers with shifts of 43, 31, and 42 cm^{-1}, respectively, while the minor population D and E conformers are both *cis*-amides with shifts of 103 and 88 cm^{-1}. These assignments are consistent with previous work by Simons and co-workers on *N*-phenylformamide[7] and *N*-benzylformamide,[4] where the *cis/trans* amide NH stretch frequencies are 3441/3463 cm^{-1} and 3443/3478 cm^{-1}, respectively.

Having assigned MEL A, B, and C as *trans*-amide conformers, it remains to assign the three to specific *trans*-amide conformational isomers. A close inspection of the frequency shifts in Table 3 suggests that they can also provide a basis for distinguishing between the various positions of the *N*-acetyl group relative to the indole ring, gauche versus anti. Of the three *trans*-amide conformers, MEL B has a shift of only 31 cm^{-1}, while that for MEL A and C are about 10 cm^{-1} greater, at 42 and 43 cm^{-1}, respectively. As Table 3 indicates, the calculations predict that the gauche *N*-acetyl positions (Gpy and Gph) have amide NH stretch fundamentals that are about 10 cm^{-1} lower than the corresponding anti position. The amide NH stretch fundamental is shifted down in frequency in the gauche position by virtue of a weak interaction of the amide NH with the π cloud of indole, which is not possible in the extended anti *N*-acetyl position. Thus, the comparison between calculation and experiment indicate that two of the *trans*-amide conformers are gauche *N*-acetyl conformers (A and C), and one (conformer B) is an anti *N*-acetyl conformer.

Further support for the assignment of conformer A to a gauche conformer and conformer B to an anti conformer comes from the R2PI spectra of conformers A and B. MEL A has substantially greater Franck−Condon intensity in the low-frequency vibrations than conformer B, consistent with its

Table 2. Summary of UV Transition Assignments in the 2C-R2PI and LIF Spectroscopy of MEL

species	frequency (cm^{-1})	relative frequency (cm^{-1})[a]	normalized intensity[b]
conformer A	32614	0	100.0
	32647	33	51.1
	32659	45	10.4
	32679	65	8.3
	32790	176	1.8
	32795	181	1.8
	33006	392	3.1
	33089	475	2.7
	33116	502	31.0
	33149	535	4.7
	33318	704	4.3
	33322	708	2.9
	33329	715	4.1
	33336	722	4.1
	33369	755	2.2
conformer B	32621	0	49.2
	32662	41	4.2
	32708	87	1.0
	33005	384	0.7
	33012	391	1.2
	33075	454	1.1
	33116	495	3.5
	33127	506	18.9
	33292	671	2.9
	33307	686	3.8
	33369	748	2.3
	33375	754	1.2
conformer C	32795	0	5.0
conformer D	32483	0	3.7
conformer E	32432	0	0.5

[a] Frequency shifts of vibronic bands of a given conformer are relative to its origin transition. [b] Peak intensities are relative to the conformer A origin, which is arbitrarily set to 100.

Table 3. Experimental and Becke3LYP/6-31+G*(5d) Calculated Frequency Shifts between the Position of the Indole NH Stretch and the Amide NH Stretch for Each MEL Conformation

conformer	assignment	experimental frequency shift (cm^{-1})	calculated frequency shift (cm^{-1})
MEL A	Gpy(*trans*-in)/anti	43	50
MEL B	Anti(*trans*-out)/anti	31	41
MEL C	Gph(*trans*-in)/anti	42	51
MEL D	Gph(*cis*-in)/anti	103	94
MEL E	Gpy(*cis*-out)/anti	88	91

assignment to a gauche conformer, in which the *N*-acetyl group interacts with the indole π cloud, and can respond to electronic excitation of the indole ring to change its position, thereby turning on Franck−Condon progressions in the low-frequency rocking vibrations of the side chain.

On the basis of energetics (Table 1), the three lowest-energy conformers (Anti(*trans*-out)/anti, Gpy(*trans*-in)/anti, and Gph-(*trans*-in)/anti) have relative energies of 0.00, 0.58, and 0.72 kcal/mol, while the next highest *trans*-amide structure (Anti-(*trans*-out)/anti) is at 1.50 kcal/mol, almost 0.8 kcal/mol higher than the other three. As a result, we anticipate on the basis of the calculations that these lowest three *trans*-amide structures are those observed experimentally. Furthermore, two of these three lowest-energy *trans*-amide conformers are gauche *N*-acetyl conformers, while the third is an anti structure, consistent with the deductions based on the amide NH stretch frequencies. We therefore assign conformer B to the Anti(*trans*-out)/anti structure and conformers A and C to the lowest energy Gpy and Gph structures.

The present experimental results cannot easily distinguish which gauche conformer (A or C) to assign to which gauche position, Gpy or Gph. On the basis of energetics, we tentatively assign conformer A to the Gpy(*trans*-in)/anti structure, which is 0.58 kcal/mol above the global minimum, and conformer C to the Gph(*trans*-in)/anti structure, with a slightly higher energy of 0.72 kcal/mol. However, the calculations cannot be depended on to faithfully reproduce this small energy difference, and future work may come to the opposite conclusion. Rotational analysis should be capable of distinguishing between these possibilities.

On the basis of the greater intensity of the transitions of MEL A relative to B, it is probable that conformer A is lower in energy than conformer B. However, the assignment of conformer A is to a gauche conformer which is higher in energy by 0.58 kcal/mol than the Anti(*trans*-out)/anti global minimum assigned to B. This may be some indication that the calculations are not yet fully converged, even at the LMP2/aug-cc-pVDZ(-f) level of theory. Full geometry optimizations (rather than the present single-point calculations) may lead to a further shuffling of the energies of the low-energy conformers of MEL. Equally important, as Godfrey et al. have recently pointed out,[10] differences in free energy between the conformers may skew the populations from that based on energetics alone. Furthermore, the cooling of population out of higher energy conformers into A and B may also effect the observed populations downstream in the expansion.

There is an alternative assignment for the three *trans*-amide conformers A−C that deserves brief mention. We stated previously that conformers A and B have $S_1 \leftarrow S_0$ origins very close to one another, while conformer C is shifted about 200 cm^{-1} to the blue. Since the 5-methoxy group is responsible for much of the large frequency shift of the $S_1 \leftarrow S_0$ origin of MEL from that of bare indole, one might wonder whether conformers A and B could be anti-methoxy structures, while conformer C is a syn-methoxy structure with a smaller electronic frequency shift.

A previous R2PI study by Sulkes and co-workers[43] led these authors to conclude that there was only one conformer of 5-MOI present in the expansion. However, 5-hydroxyindole has two $S_1 \leftarrow S_0$ origins because of syn and anti hydroxy isomers, separated from one another by 228 cm^{-1}.[46,47] Furthermore, no

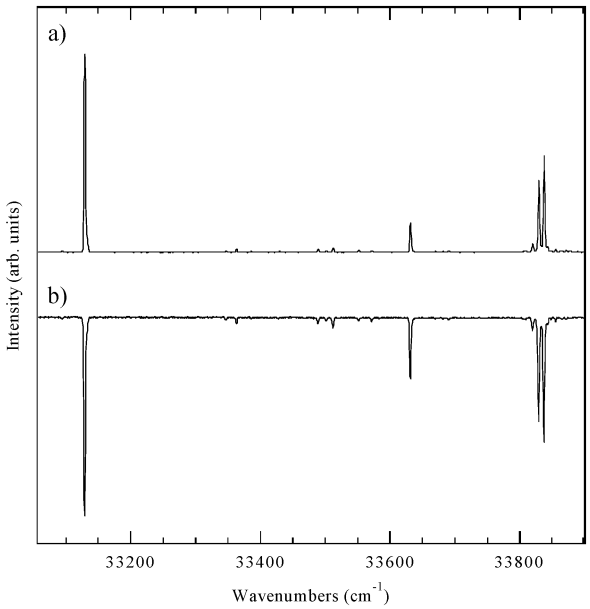

Figure 8. (a) LIF scan of 5-methoxyindole in the region of the $S_1 \leftarrow S_0$ origin. (b) UV−UV hole-burning scan taken with hole-burn laser tuned to the origin at 33130 cm^{-1}. The hole-burn scan demonstrates that all structure in the LIF spectrum arises from a single-ground-state level, assignable to the anti-methoxy conformer based on energetics.

hole-burning studies were conducted in the previous work on 5-MOI to address the question of conformational isomers directly. As a result, we carried out LIF and UV−UV hole-burning spectroscopy on 5-MOI. The results, shown in Figure 8a and 8b, prove that all the transitions observed in the LIF spectrum are due to a single conformer of 5-MOI. Calculations we preformed at the Becke3LYP/6-31+G*(5d) level of theory indicate that the barrier to isomerization from syn to anti 5-MOI is 1.4 kcal/mol while the syn 5-MOI minimum is about 1 kcal/mol above the anti minimum. On the basis of these calculations, it seems likely that the preexpansion population in syn-oriented 5-MOI can be converted into the anti conformer via collisions with the buffer gas in the expansion. By analogy, unless the side chain in the 3-position of MEL effects either the relative energies of the syn and anti methoxy isomers or the height of the isomerization barrier separating them substantially, it seems unlikely that conformer C of MEL can be attributed to a syn-methoxy isomer.

We have yet to assign conformers D and E to specific *cis*-amide structures. On the basis of the relative intensities of the transitions in the R2PI and LIF spectra, conformer D is anticipated to be lower in energy than conformer E. Furthermore, our experience with the *trans*-amide conformers would suggest that the lower frequency of the amide NH stretch for conformer D (3420 cm^{-1}) relative to conformer E (3435 cm^{-1}) might result from the former structure incorporating the amide NH group in a weak π H-bond not experienced by conformer E.

We have not done an exhaustive search for *cis*-amide structures. However, the lowest energy *cis*-amide structures found in our work are the Gph(*cis*-in)/anti and Gpy(*cis*-out)/anti structures with energies 2.92 and 3.27 kcal/mol above the global minimum, at the DFT B3LYP/6-31+G*(5d) level of theory (Table 1, Figure 2). Furthermore, the Gph(*cis*-in)/anti structure points the amide NH group in toward the indole π

(47) Sulkes, M., 2001. Personal communication.

cloud, while the Gpy(*cis*-out)/anti orients the NH group away from indole. This suggests that conformer D be assigned to the Gph(*cis*-in)/anti structure and conformer E to the Gpy(*cis*-out)/anti conformer. However, the calculated frequencies of the amide NH stretch fundamentals (Table 3) do not show the expected frequency ordering, and no firm assignment to specific *cis*-amide structures can be made on the basis of the present data.

IV. Discussion

The Conformational Preferences of Melatonin. In this work, the methods of mass-selected resonant two-photon ionization, laser-induced fluorescence excitation, UV−UV hole burning, resonant ion-dip infrared spectroscopy, and fluorescence-dip infrared spectroscopy have been used to determine the conformational preferences of melatonin in the gas phase. By studying the isolated molecule under jet-cooled conditions, well-resolved ultraviolet transitions due to five conformations are observed. The double-resonance methods of UV−UV hole burning, RIDIR spectroscopy, and FDIR spectroscopy have been used to acquire the UV and IR spectra of each of the five conformations free from interference from the others present in the expansion.

Not unexpectedly, the three dominant conformations are all *trans*-amide structures. As in other tryptophan analogues, the preferred orientation of the ethyl side chain is nominally perpendicular to the indole ring, leading to three distinct positions for the *N*-acetyl group: gauche on the pyrrole side of indole, gauche on the phenyl side, and anti. Our assignment of conformers A−C shows that population is present in all three positions, with some preference for the Gpy and anti structures over the Gph structure. The low-energy gauche structures point the amide NH group in toward the π cloud, consistent with formation of a weak π H-bond. This is borne out by the spectroscopy of the Gpy and Gph conformers, in which the amide NH is shifted down in frequency by 15 and 13 cm^{-1}, respectively, relative to the anti structure. According to the calculations, the methoxy group in the 5-position is in-plane and prefers an orientation anti with respect to the indole NH, rather than syn. Unfortunately, the calculations show little difference in the methoxy methyl CH stretch frequencies in the two orientations, and we are left to surmise an anti structure for the methoxy group on the basis of the calculated energetic preference for this orientation. However, the calculated energy difference between corresponding syn- and anti-methoxy structures is rather large (~3 kcal/mol at the LMP2/aug-cc-pVDZ(-f) level of theory), leaving little doubt that the methoxy group prefers the anti structure, as in the related 5-MOI molecule.

The fourth and fifth conformers, whose $S_1 \leftarrow S_0$ origin intensities are only 5 and 1% that of conformer A, have been assigned to *cis*-amide structures. The present data provides no firm assignment for which *cis*-amide structures are observed, leaving largely open the question of how the preference for gauche and anti *N*-acetyl groups is changed by the amide conformation. What is clear, however, is that these *cis*-amide structures are observed when several others with energies similar to or below them are not. It is this issue to which we now turn.

Conformational Cooling and Population Trapping in the Supersonic Expansion. In most previous studies of conformationally flexible biomolecules, the primary criterion used to decide which conformational minima were potential candidates for experimental observation was the energy of the minima relative to one another. In comparing two conformers, the one with lower energy is generally preferred. However, the detection of two *cis*-amide conformers in melatonin presents a clear exception to this rule, raising the following questions:

(1) Why are the *cis*-amide conformers observed despite their high energy?

(2) Why are several *trans*-amide or syn-methoxy conformers not observed, despite the fact that they are lower in energy than the *cis* conformers?

One potential solution to both these questions is simply to call into question whether the calculations correctly reproduce the experimental energies of the conformers. Issues of intramolecular basis set superposition error, the lack of dispersion in the DFT calculations, and the use of a modest-sized basis set all point to the need for higher level calculations to address these issues. This motivated our single-point localized MP2/aug-cc-pVTZ(-f) energy calculations which did show considerable differences from the DFT results and which highlight the need for full optimizations at the LMP2 level of theory to further address this point. However, while the LMP2 calculations did change the relative energies of the conformers, they did not change the qualitative picture and general energy ordering of the structures, making it unlikely that arguments based on the relative energies of the conformational minima will answer the above questions satisfactorily.

Instead, the populations of the conformers of MEL observed downstream in the expansion reflect both the energies of the minima and the barriers to isomerization separating them. Thus, the presence of two *cis*-amide conformers can only be accounted for once the large barrier to *cis/trans* isomerization about the amide bond is recognized. The preexpansion conformer population is in full thermal equilibrium. One anticipates, then, a *cis*-amide Boltzmann population prior to expansion that reflects this energy difference. Using an energy difference of 3 kcal/mol and a temperature of 200 °C, the total population in MEL D should be ~4% that of the *trans*-amide global minimum. Assuming that population alone determines the relative intensities of the LIF and R2PI origin transitions, this estimate agrees well with the experimental value of ~5%, determined from the LIF intensity ratio of MEL D to MEL A. Thus, it appears that the Boltzmann population in *cis*-amide conformations is effectively trapped there by the large barrier to *cis/trans* isomerization and cannot be removed by the cooling collisions in the expansion. In retrospect, this is not surprising in light of the magnitude of the barrier to *cis/trans* isomerization (15−20 kcal/mol).[11−13] The short time scale of the expansion and the small collision energies available in the expansion cannot overcome such a barrier during the cooling process.

At the same time, the expansion is remarkably effective in collapsing all the *cis*-amide population into two minima and the *trans* population into three minima. One cannot allow the presence of a *cis* population of a few percent of the global minimum without recognizing that the many other *trans* minima calculated to be lower in energy than these *cis* conformers must have had measurable populations in them prior to expansion. The syn-methoxy counterparts of conformers A−C are cases in point. These conformers have similar energies to the *cis*-

amide conformers, yet they are not observed, while the *cis*-amide conformers D and E are readily detected. Given the excellent signal-to-noise ratio of the LIF scan of Figure 3 and the R2PI scan of Figure 4, conformational origins of about 0.1% of A or B should have been observable. Our calculations on 5-MOI indicate that there is a barrier to isomerization out of the syn-methoxy conformer of about 1.4 kcal/mol, which is small enough that collisions may be able to remove this population as cooling occurs in the expansion. By analogy, we anticipate the barrier out of syn-methoxy MEL conformers to be small as well.

There are several previous studies of conformationally flexible molecules that have addressed the magnitudes of the barriers needed to trap population in local minima.[1−3,8−10] In molecules that contain two conformational minima and a single isomerization coordinate, the rule of thumb that developed from the early studies is that a barrier of at least 400 cm^{-1} (1.1 kcal/mol) is needed to trap population in a neon expansion. In tryptamine and 3-indole-propionic acid, which have two low-energy flexible coordinates, this rule appears to have been followed in large measure.[1−3] More recent studies[9,10,19] on molecules with several flexible coordinates have shown that the barrier required to trap population in the expansion is increased to about 1000 cm^{-1} (2.9 kcal/mol) in these larger molecules because of the larger internal energies available to the molecules prior to expansion and the higher preexpansion temperatures used. As a result, as Godfrey et al. have pointed out,[9,10] a proper account of the expansion-cooled populations must consider not only the conformational minima but also the connectivity of the potential energy landscape (e.g., which minima are connected to which), the magnitudes of the barriers separating the minima, the Boltzmann populations prior to expansion (which are determined by the free energies of the conformations), and the dynamics of cooling on the potential energy landscape.

In MEL, we have direct experimental evidence that the population of MEL C is smaller in a 70% neon/30% helium expansion than in a pure helium expansion, demonstrating the importance of cooling collisions in effecting the downstream population of this conformer. However, transition-state structures, isomerization pathways, and their energies are not yet available for MEL, especially at a level of theory where they can be considered reliable. Such an exploration of the potential energy landscape is a rather daunting task. On the basis of experience with other molecules, it seems likely that the magnitudes of the conformational barriers separating the low-energy minima of MEL will be similar to that in tryptamine or 3-indole propionic acid, where barriers of 500 to 1000 cm^{-1} were typical. Clearly, a more thorough knowledge of the potential energy landscape for MEL will be required before a firm answer regarding specifics of conformational cooling in the expansion can be given.

The Relevance of Gas-Phase Conformations to Melatonin Binding at the Receptor Site. One of the motivations for studying the conformational preferences of melatonin in the gas phase is that it may help us understand its preferred conformations in aqueous solution and when bound to membrane receptor sites in the brain. Clearly, melatonin may have different conformational preferences in each of these environments. Yet, it is precisely this type of comparison that is not typically available. With it, it may be possible to assess the effects of aqueous solvent and of the receptor site itself, as further data on the conformations of melatonin in these environments becomes available.

In the gas phase, the Anti(*trans*-out)/anti and Gpy(*trans*-in)/anti structures are the two most stable conformations (Figure 2, Table 1), but all three positions for the *N*-acetyl group are relatively close in energy to one another. According to the calculations, almost all the low-energy structures of MEL have the C(α)−C(*β*) bond nearly perpendicular to the indole ring. However, there are a few low-energy conformations that place this bond in the plane of the indole ring. The lowest of these is only 1.14 kcal/mol above the global minimum (Figure 2). Similarly, the methoxy group prefers an in-plane structure that points the methyl group toward, rather than away from, the *N*-acetyl ethylamine side chain. The energy difference here is about 3 kcal/mol. The difference in energy between conformational families involving the amide bond, *cis* versus *trans*-amides, is also about 3 kcal/mol. Energy differences of this scale are about five times *kT* at room temperature (0.6 kcal/mol). Such *cis* structures seem not to be seriously considered in biological models of melatonin binding.[14,16−18,48]

It would seem that the conformational preferences of melatonin are played out on rather modest energy scales that are comparable to, or somewhat greater than, *kT*. Likely, energy differences of this magnitude can be overcome readily by hydrogen bonds with water in aqueous solution. It would be interesting to determine the conformational preferences of melatonin in aqueous solution for comparison with the present gas-phase results. To probe the beginnings of such solvation, we are currently studying the spectroscopy of the water-containing clusters of melatonin.[42]

Without a strong, intrinsic structural preference, it seems likely that nature may use these small energy differences and modest energy barriers (<5 kcal/mol) to enable melatonin to deform into the desired shape for binding as it enters into or moves within the receptor binding pocket. It also may facilitate the binding of melatonin to different types of receptor sites in carrying out its multiple biological functions. In fact, as we have suggested previously,[49] the formation of a hydrogen bond to the binding site could provide a source of energy for the rearrangement into the desired configuration.

Even the preference for *trans* over *cis*-amide conformations is not of a size so large as to make it alone the reason that *cis*-amide structures are not likely candidates for binding to the receptor. One could imagine circumstances under which better binding by the *cis* conformation to the receptor could compensate for the 3 kcal/mol energy difference in a receptor of the right design. Instead, it seems more likely to us that the preference for *trans* over *cis* structures derives in some measure from the large barrier to *cis/trans* isomerization of the amide bond. This large barrier could prevent isomerization on the encounter time scale in the binding pocket. This would give an element of kinetic control to the binding.

V. Conclusions

The present investigation has probed the conformational preferences of melatonin by studying the infrared and ultraviolet

(48) Spadoni, G.; Mor, M.; Tarzia, G. *Biol. Signals Recept.* **1999**, *8*, 15.
(49) Carney, J. R.; Dian, B. C.; Florio, G. M.; Zwier, T. S. *J. Am. Chem. Soc.* **2001**, *123*, 5596.

spectra of individual conformations in the isolated molecule under jet-cooled conditions. The detection of two *cis*-amide conformations and the conspicuous absence of many conformations of equal or lower energy show clearly that small populations can be trapped behind large barriers on the time scale of collisional cooling in the expansion. The five conformers show unique amide NH stretch fundamentals. The *trans*-amide anti conformer (MEL B), in which the amide NH is free, has its NH stretch fundamental at 3495 cm^{-1}. The *trans*-amide gauche structures (MEL A and C) point the amide NH in toward the indole π cloud, producing 15 and 13 cm^{-1} shifts down in frequency to 3480 and 3482 cm^{-1}. The *cis*-amide structures have amide NH stretch fundamentals shifted to lower frequency than their *trans*-amide counterparts, providing a definitive signature for their presence. The gauche pyrrole MEL E structure has the amide NH away from the ring and results in a free NH stretch frequency of 3435 cm^{-1}. Finally, the *cis*-amide gauche phenyl structure (MEL D) NH fundamental points the amide NH in toward the indole π cloud, producing a 15 cm^{-1} red shift to 3420 cm^{-1}.

While these studies have probed the preferred conformational minima of melatonin, they also point out the need for both experimental and theoretical studies that probe the barriers to and preferred pathways for conformational change in molecules of this size. It is also hoped that the present data can serve as a testing ground for higher-level ab initio calculations and improved molecular mechanics force fields.

Acknowledgment. T.S.Z. and G.M.F. gratefully acknowledge the National Science Foundation Experimental Physical Chemistry Program for their support of this work under a two-year creativity extension to grant CHE9728636. G.M.F. thanks the Purdue Research Foundation for a graduate student fellowship. The authors acknowledge the assistance of Dr. Asier Longarte, Brian Dian, and Dana Holcomb.

Supporting Information Available: Table listing Becke3LYP/6-31+G*(d) calculated infrared frequencies and intensities of select MEL conformations (PDF). This material is available free of charge via the Internet at http://pubs.acs.org

JA0265916